Functional Diamond

ISSN: 2694-1112 (Print) 2694-1120 (Online) Journal homepage: www.tandfonline.com/journals/tfdi20

Diamond as the heat spreader for the thermal dissipation of GaN-based electronic devices

Liwen Sang

To cite this article: Liwen Sang (2021) Diamond as the heat spreader for the thermal dissipation of GaN-based electronic devices, Functional Diamond, 1:1, 174-188, DOI: 10.1080/26941112.2021.1980356

To link to this article: https://doi.org/10.1080/26941112.2021.1980356

Published online: 15 Oct 2021.

FUNCTIONAL DIAMOND
2021, VOL. 1, NO. 1, 174–188
https://doi.org/10.1080/26941112.2021.1980356

Taylor & Francis
Taylor & Francis Group

REVIEW

Diamond as the heat spreader for the thermal dissipation of GaN-based electronic devices

Liwen Sang[a,b]

[a]International Center for Materials Nanoarchitectonics (MANA), National Institute for Materials Science (NIMS), Tsukuba, Ibaraki, Japan; [b]JST-PRESTO, The Japan Science and Technology Agency, Tokyo, Japan

ABSTRACT

With the increasing power density and reduced size of the GaN-based electronic power converters, the heat dissipation in the devices becomes the key issue toward the real applications. Diamond, with the highest thermal conductivity among all the natural materials, is of the interest for integration with GaN to dissipate the generated heat from the channel of the AlGaN/GaN high electron mobility transistors (HEMTs). Current techniques involve three strategies to fabricate the GaN-on-diamond wafers: bonding of GaN with diamond, epitaxial growth of diamond on GaN, and epitaxial growth of GaN on diamond. As a result of the large lattice mismatch and thermal mismatch, the integration of GaN-on-diamond wafer is suffered from stress, bow, crack, rough interfaces, and large thermal boundary resistance. The interfaces with transition or buffer layers impede the heat flow from the device channel and greatly influence the device performance. In this review, we summarize the three different techniques to achieve the GaN-on-diamond wafers for the fabrication of AlGaN/GaN HEMTs. The problems and challenges of each method are discussed. In addition, the effective thermal boundary resistance between GaN and diamond, which characterizes the heat concentration, is analyzed with regard to different integration and measurement methods.

ARTICLE HISTORY
Received 13 June 2021
Accepted 26 August 2021

KEYWORDS
Semiconductor;
Heat-related

1. Introduction

Benefitted from the high breakdown voltages (10 times higher than Si), high switching speed (over GHz), compact size, and tunable electronic architecture [1–7], III-V nitride semiconductor is becoming one of the best candidates for high-power electronics to enable the increasing power density and high conversion efficiency. The commercialized AlGaN/GaN high electron mobility transistors (HEMTs) have led to the entry into the medium-power market, and play a central role for the RF and millimeter-wave applications [8–11]. In the applications of 5 G communications, radar, and electronic warfare, the HEMTs devices can offer more than 10 times higher power density than the existing Si technologies [12]. This giant power induces a huge amount of heat in the chip area, creating localized hot spots with fluxes above 10 kW/cm^2 and package-level volumetric heat generation that can exceed 100 W/cm^{-3}. The high-level power dissipation results in the challenges using conventional approaches for the thermal management. With the increased power density, self-heating inside the devices becomes an essential issue that accelerates the failure and poor reliability in the real application. Thermal dissipation through conventionally used approaches is no longer adequate. To achieve the effective thermal dissipation, the heat spreader with a much higher thermal conductivity is required.

The current GaN wafers are typically grown on sapphie, silicon (Si), silicon carbide (SiC), or free-standing GaN substrates, whose thermal conductivities are 35, 150, 400, and 280 W/mK, respectively [13–15], which are far from the requirements. The ideal heat spreader would be a substrate that is both highly thermally conductive and electrically insulating. Diamond, with the thermal conductivity up to 2400 W/mK at room temperature for the single crystals, and approaching 2000 W/mK for the polycrystals, is the best candidate as a heat spreader for GaN power transistors [16–19]. Early simulations and modelling showed that the passive thermal extraction by direct contact with diamond could dramatically reduce junction temperatures by 25-50% [20–23]. However, as shown in Table 1, diamond and GaN exhibit widely mismatched properties, such as the crystalline structures, lattice constants and thermal expansion coefficients (TEC), making them challenging as bonded or growth pairs [24–28].

CONTACT Liwen Sang SANG.Liwen@nims.go.jp

Over the past twenty years, a variety of methods have been developed to utilize diamond as the heat spreader for AlGaN/GaN power transistors. The developed wafer is therefore called "GaN-on-diamond wafer". The approaches are summarized in Figure 1, which include: (1) bonding of diamond to GaN wafers or directly to the HEMT devices with/without an adhesion layer, (2) GaN epitaxial growth on single-crystal or poly-crystal diamond substrate, then fabrication of HEMT devices, and (3) nanocrystalline or poly-crystalline diamond growth on the frontside or backside of GaN or the HEMTs devices. For the three approaches, the thermal resistance at the GaN/diamond, which is referred to the "effective thermal boundary resistance (TBR_{eff})", is one of the factors that significantly increases the overall temperatures during device operation. Therefore, the optimizations on the integration technique and interface property are important. In this review, the state-of-the-art development on the GaN-on-diamond wafer and the modified fabrication process for HEMTs with regard to different integration methods will be presented. The strategies to improve the interfaces and reduce the TBR_{eff} will be summarized and discussed. The device performances will be further shown with respect to different methods.

Table 1. The lattice constant and thermal expansion coefficient of GaN, sapphire, Si and diamond at room temperature.

Substrate	GaN (a-axis)	Sapphire	Si	Diamond
Lattice constant (Å)	3.189	4.758	5.420	3.567
TEC ($\times 10^{-6}K^{-1}$)	5.6	4.5-5.8	2.6	~1.1

2. Integration of the diamond to GaN or HEMTs through bonding technique

The concept of harvesting the III-V epitaxial layers from one substrate and thermally bonding them to another

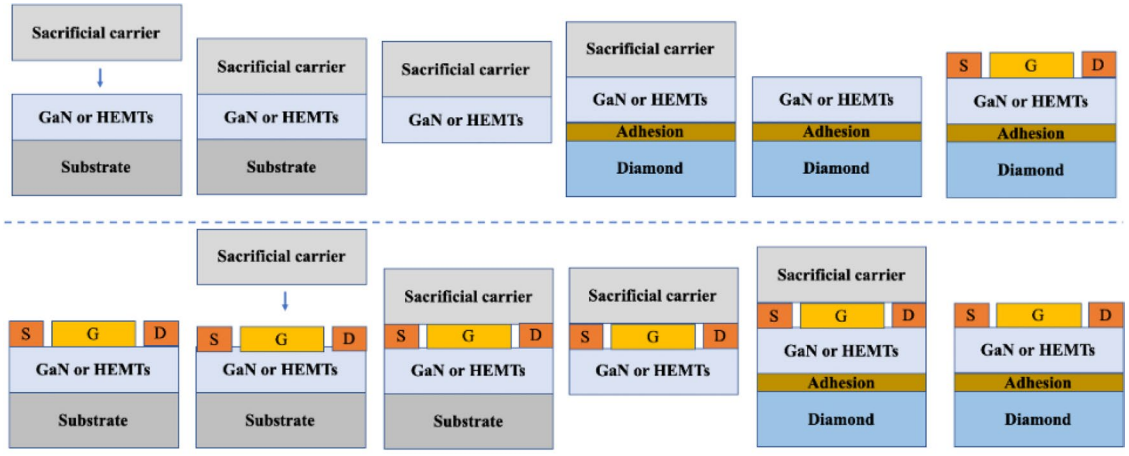

(a) Top: GaN wafer bonding to diamond then fabricate HEMT devices; Bottom: HEMTs devices directly bonding to diamond substrate

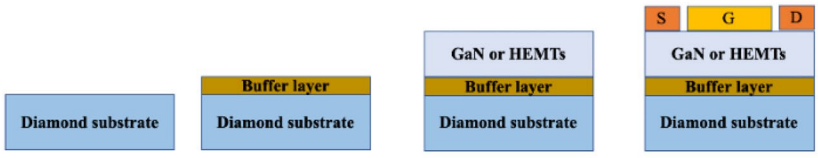

(b) HEMT devices epitaxial grown on diamond substrate

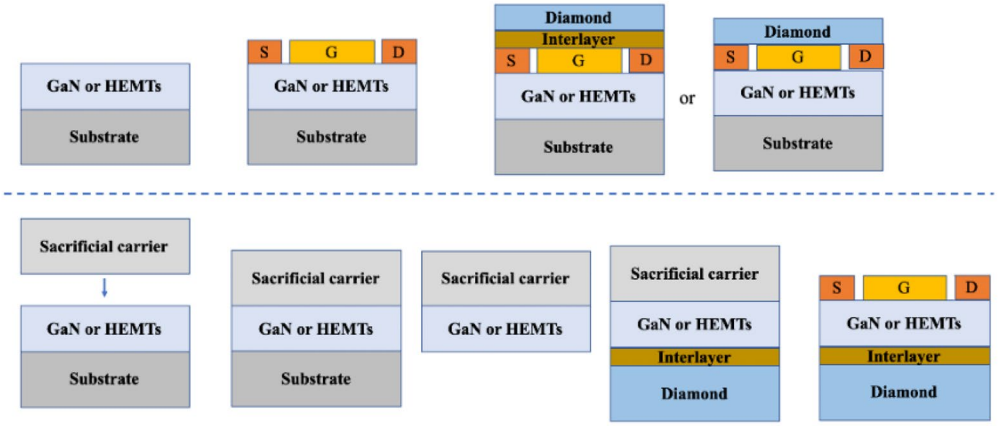

(c) Top: Diamond grown on the top of HEMTs devices; Bottom: Diamond epitaxially grown on HEMT wafers

Figure 1. Fabrication of the GaN-on-diamond wafer for the HEMT devices.
S: source, D: Drain, G: gate.

substrate was proposed in the 1990s [29,30]. In 1997, Kelly *et al.* firstly demonstrated the lift-off of GaN film from sapphire substrate by illuminating the interface with a pulsed laser [31], which enabled the development of the GaN bonding technology. With the development of GaN-on-Si technology [32,33], the bonding process of GaN or HEMTs wafer became much easier due to the easy removal of the Si substrate. The advantage for the GaN bonding to diamond is that the crystal quality of both GaN and diamond can be guaranteed after the bonding.

The formation of GaN-on-diamond wafer started with GaN or AlGaN/GaN HEMT epitaxial layers grown on a silicon substrate [34]. Other substrates, such as sapphire, silicon carbide, or aluminum nitride may also be used. In order to preserve the orientation of the epilayers, which is required to fabricate HEMTs on this structure, the epilayer was transferred twice (Figure 1 (a) top). The GaN-epilayer structure was firstly bonded to another sacrificial carrier. The growth substrate was then removed using either a wet chemical or dry etching process that is selective to GaN, leaving GaN epilayers flipped. An atomically flat dielectric layer was then deposited to bond with the diamond. The sacrificial carrier wafer was finally removed, leaving a composite wafer in which the GaN epilayers were attached to the diamond substrate. In this case, diamond was bonded to the N-polar HEMT devices. This process maintains the growth direction and the orientation of the built-in polarization fields of the GaN HEMTs for the realization of the 2D electron gas (2DEG). However, due to the bowing of the wafer, the optical lithography was unavailable for the process while an electron beam lithography was utilized for the device fabrication. Silicon nitride (SiN_x), with a low thermal conductivity, was the typical adhesive dielectric layer, the heat barrier therefore was mainly located at the interface between GaN and diamond.

Since the GaN used in this process can be grown on Si substrate, in principle, this process can be scaled to wafers of any size. But the wafer bow and wafer cracks resulted from different stresses during the formation of GaN-on-diamond wafer greatly limit the wafer size. Except for the lattice mismatch between the film and substrate, the thermal stress is also a well-known challenge. The thermal stresses arise due to the thermomechanical properties of the layers in the stack [35], the differences in the thermal expansion coefficients. The stresses bowed and/or warped the wafers as they cooled down from the process temperature to room temperature. By 2007, this process was improved and the 2-inch diameter GaN-on-diamond wafer was produced. In 2009, Francis *et al.* published the first demonstration of a 4-inch GaN-on-diamond wafer, as shown in Figure 2 [34, 36]. The interface between GaN and diamond through the adhesive layer was characterized by the acoustic properties using picosecond laser-ultrasonic probing. The measurement indicated a good adhesion of the interlayer to both GaN and diamond. The GaN-on-diamond wafer technology has been demonstrated with 80 to 100 μm thick diamond substrates, which are mechanically stronger and flatter than that of the thin wafers. The developed GaN-on-diamond substrates were then utilized for the fabrication of devices, which demonstrated transition frequencies up to 85 GHz [37]. A comparison of device performances between GaN-on-silicon and GaN-on-diamond was reported, which confirmed that the bonding process could avoid the damage to the active region of HEMTs [38]. The fabricated GaN HEMT-on-diamond transistor had a power density of 2.79 W/mm at 10 GHz. The device on SiC had a number of dimensional variables in its favor and demonstrated twice the thermal resistance of that on GaN-on-diamond. By using GaN-on-diamond as opposed to GaN-on-SiC, the operating junction temperature was reduced by 40-45% (Figure 3), and the thermal improvement has tripled the areal RF power density from a GaN transistor. However, the relatively low current densities in the GaN-on-diamond devices limited the output power compared to the devices on

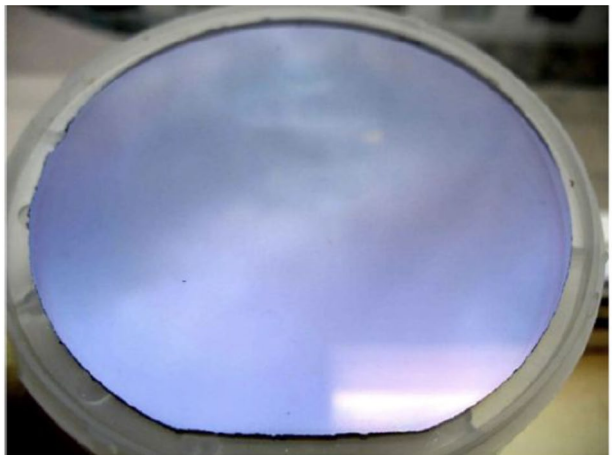

Figure 2. Photograph of a 4-inch GaN-on-diamond wafer [34].

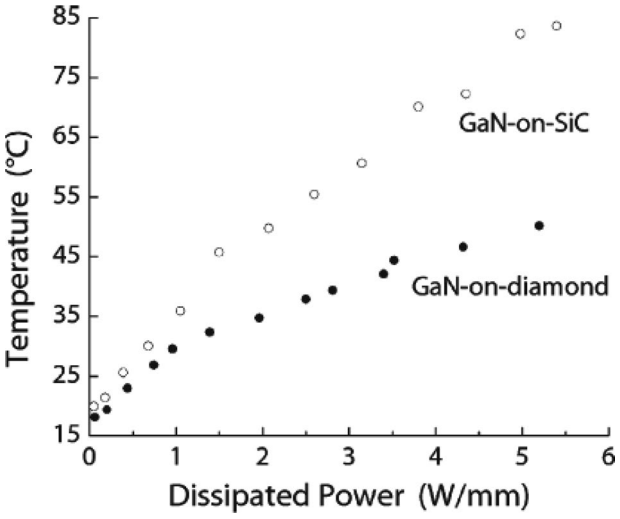

Figure 3. The operating temperature of the GaN-on-diamond and GaN-on-SiC HEMTs [38].

GaN-on-SiC (Figure 4), which may be attributed to the trapping effects rather than the heating effect.

To avoid the heat barriers caused by the adhesive dielectric layer, the direct bonding without adhesive agent was developed. J. C. Kim *et al.* used a spark plasma sintering process at 1000 °C with a uniaxial pressure to fabricate the GaN-on-diamond wafers [39]. The high-resolution transmission electron microscopy (HRTEM) confirmed the formation of GaN on diamond *via* the chemical bonding. Unfortunately, the localized hot molten zones of interlayer were observed during the spark plasma environment, bringing out the difficulty using this method.

The high temperature process in the bonding approaches leads to the considerable stress and the wafer bowing due to the large mismatch of TEC. Besides, the high temperature process may also induce chemistry modification and damages of the bonded structure. To overcome these issues, a low temperature bonding technique was developed. The low temperature wafer bonding is successful in various applications such as the fabrication of silicon-on-insulator (SOI), heterogeneous integration, and advanced packaging at temperature below 400 °C [40,41]. One approach at room temperature is to employ the surface activated bonding machine, in which the Ar ion beam at high power was used to active both the surfaces and a Si nano-layer was sputtering deposited as the adhesion layer [42]. After the surface preparations, the two samples were bonded at room temperature by contact and press. But due to the high-power Ar ion deposition, an amorphous diamond layer was formed between diamond and the deposited Si as well as between the deposited Si and GaN, as shown in Figure 5 (a) and (b) by HR-TEM [43]. To experimentally obtain the TBR_{eff} between GaN and diamond, the time-domain thermoreflectance (TDTR) was utilized, which is a pump-probe technique that can measure thermal properties of the nanostructures and epitaxial films. The TBR_{eff} between GaN and diamond using surface-activated bonding (SAB) was estimated to be ~18 m^2K/GW, corresponding to a thermal boundary conductance (TBC) of 53 MW/m^2K. When the thickness of Si was reduced to 4 nm (Figure 5 (c) and (d)), the TBR_{eff} was further reduced to ~10 m^2K/GW. However, it is noted that, the yield of the direct bonding using the above methods for the formation of GaN-on-diamond is still low for the larger wafer diameters due to the challenge of uniform polishing of the GaN layer and the bonding process. Mu *et al.* reported on the 1 cm × 1 cm sized polycrystalline diamond bonded to the GaN/sapphire [42]. Cheng *et al.* utilized the single-crystalline diamond substrate for the surface activated bonding to GaN and the size was even smaller [43].

The success of the low-temperature bonding of GaN to diamond enables the device transfer to the diamond technique. The device transfer has the direct advantage of utilizing the standard high yield GaN HEMT process. Chao *et al.* reported the GaN-on-SiC HEMTs devices transfer to the polycrystalline chemical vapor deposition (CVD) diamond substrate with a maximum drain current density of 1.2 A/mm and peak transconductance of 390 mS/mm [44]. In this approach, a thin layer of Si-based adhesion was utilized and the bonding process was at the temperature of 150 °C. It was confirmed that the GaN HEMT-on-diamond maintained lower channel temperatures than the original GaN HEMT-on-SiC while delivering 3.6 times higher RF power within the same active area. In 2017, Liu *et al.* firstly achieved the 3-inch GaN-on-diamond HEMTs device transferred to the diamond substrate at the bonding temperature of 180 °C [45]. The 3-inch device wafer was coated with a thermosetting adhesive layer, then bonded face-down onto a 3-inch SiC temporary carrier wafer. A bonding adhesion layer with a thickness of 15-20 nm was deposited onto the exposed GaN as well as on the 3-inch polycrystalline diamond substrate. For a GaN HEMT at the power dissipation of 10 W/mm, the peak junction temperature of the device was decreased from 241 °C to191 °C after transferring to the diamond substrate. A maximum current density of ~1 A/mm and a power

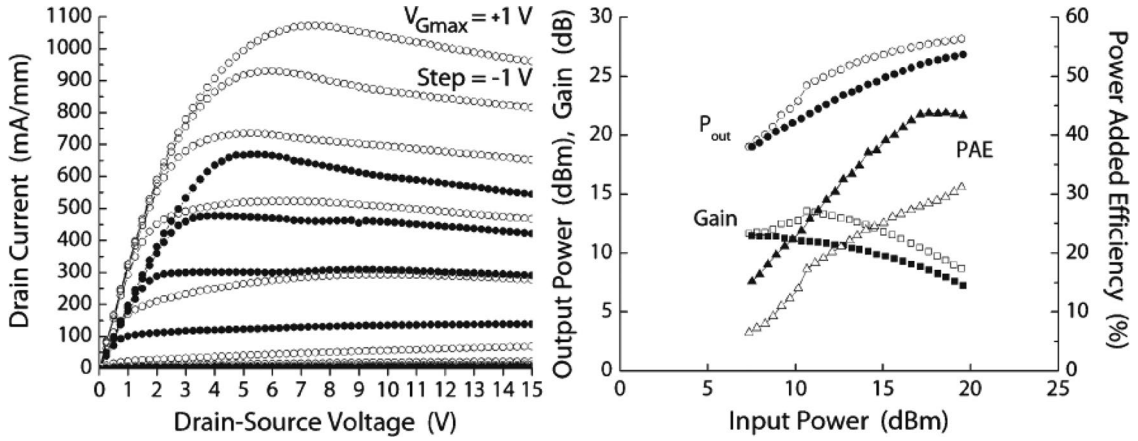

Figure 4. Electrical characteristics. (a) I-V characteristics for GaN-on-diamond (solid) and GaN-on-SiC HEMT devices (hollow). (b) output power measured at 10 GHz CW and V_{DC} = 20 Vfor for GaN-on-diamond (solid) and GaN-on-SiC HEMT devices (hollow) [38].

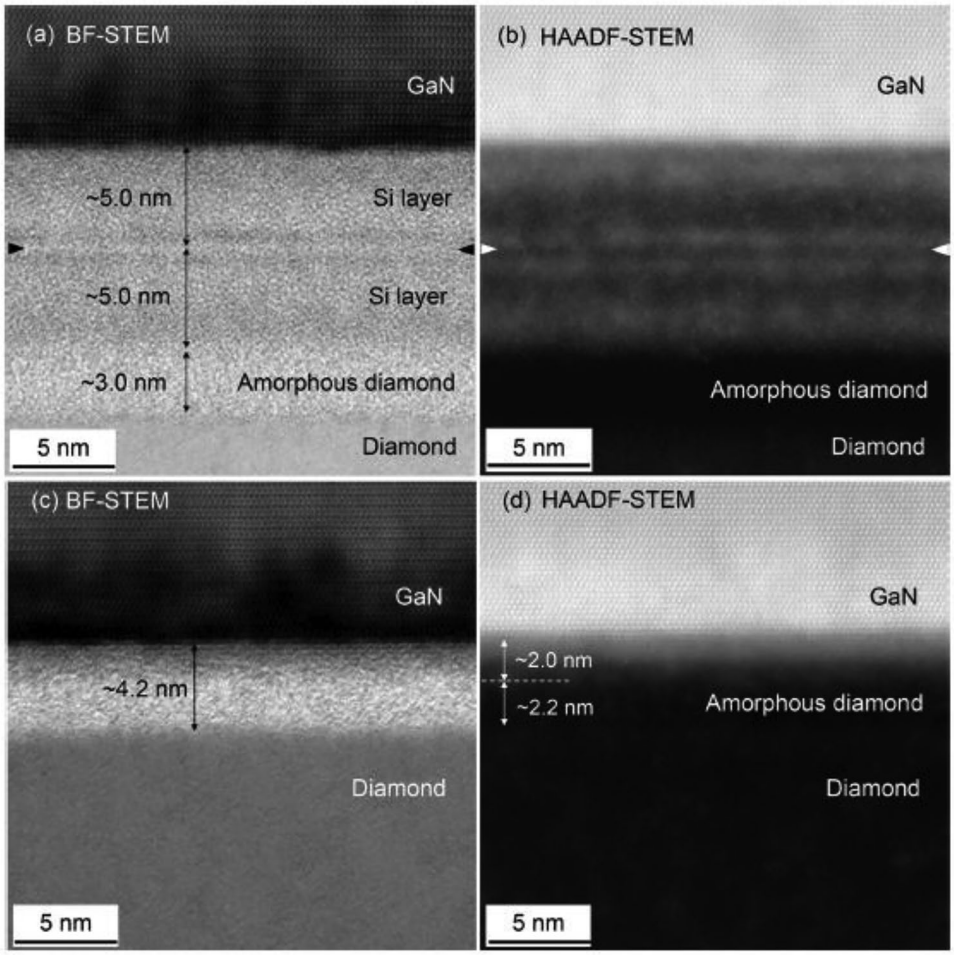

Figure 5. (a) Cross-sectional HR-TEM images and (b) high-angle annular dark field scanning TEM images of the GaN/diamond interfaces using SAB bonding. (c) and (d) are for the sample with the improved interfaces [43].

density of 5.5 W/mm CW at 10 GHz with the power added efficiency (PAE) of 50.5% were achieved (Figure 6). By using a finite-element analysis, the TBR_{eff} of 19 m^2K/GW was obtained in the GaN-on-SiC device, while the TBR_{eff} in the GaN-on-diamond was estimated to be 51 m^2K/GW. Further optimization on the thermal conductivity of the adhesion layer, thickness and bonding process is still needed.

3. Gan epitaxially grown on the diamond substrate

Another method to achieve the GaN-on-diamond is to grow the GaN and HEMT structures on the diamond substrate. The epitaxial growth is challenging due to the large lattice mismatch and thermal mismatch between GaN and diamond, as shown in Table 1. The lattice mismatch between GaN and diamond is 11.8% [46–49]. The thermal mismatch with different TECs also induces a high tensile strain in the epilayer during the cooling down of the sample after growth. There are a lot of efforts in the GaN deposited on different types of diamond substrates, such as single crystal diamond (SCD) with (110), (111) or (100) orientations, nano-crystalline diamond, polycrystalline diamond, or the highly misoriented diamond substrate [49–63]. The growth methods include metal organic chemical vapor deposition (MOCVD), molecular beam epitaxial (MBE), HVPE and resonance plasma enhanced MOCVD (ECR-MOCVD) [49–59].

The first trial of GaN deposition on the SCD substrate is in 2003. Since the GaN with the device quality can be deposited on sapphire substrates using a buffer layer, in spite of the lattice mismatch of nearly 16.1%, researchers also utilized an AlN nucleation layer to deposit GaN on the type IIa (110) SCD substrate by MOCVD [49]. However, the closely packed GaN grains instead of the smooth surface were observed on the surface. X-ray diffraction (XRD) showed the GaN layer was polycrystalline and hexagonal, with c-plane orientation perpendicular to the substrate. As a result of the carbon incorporation originating from the substrate, a very poor optical quality was determined by photoluminescence.

In 2003, the epitaxial growth of AlN layer on diamond (100) substrate was improved by plasma-induced MBE [50]. The silicon-doped n-type AlN film on the natural boron-doped p-type diamond substrate formed a hetero-bipolar diode with good rectifying properties and

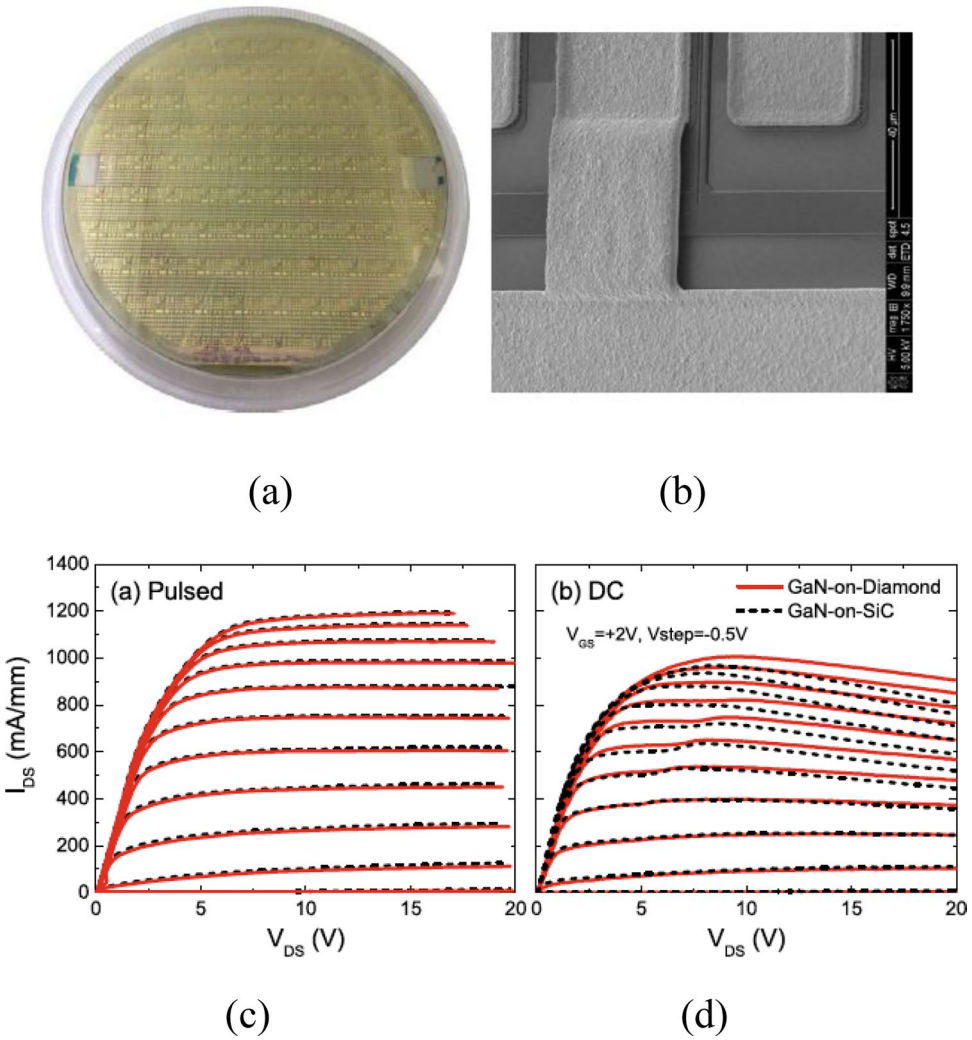

Figure 6. (a) A 3-inch GaN-on-diamond wafer by substrate transfer process, (b) SEM image of air bridge of a multi-finger device. Pulsed (c) and DC (d) I-V characteristics of GaN HEMT before (dashed lines) and after (solid lines) substrate transfer.

surprisingly efficient light emission in the spectral range from 2.7 to 4.8 eV under forward bias. The AlN was wurtzite with the [0001] direction on the diamond. However, the quality of the GaN was still unacceptable on the diamond (100) substrate. The XRD pole figure analysis established the presence of the two domains of epitaxial layer, namely (0001)<10-10>GaN//(001)[110] diamond and (0001)<10-10>GaN//(001)[1-10] diamond, which were 90° rotated with respect to each other [51]. The presence of these domains was explained by the occurrence of areas of (2×1) and (1×2) surface reconstruction of the diamond substrate. When applying highly misoriented diamond substrates toward the [110] diamond direction, one of the growth domains was suppressed and the crystalline quality of GaN was improved. However, the surface of the GaN was still rough and could not be utilized for the HEMT devices.

The quality of the GaN was improved when the SCD (111) substrate was utilized. In 2009, Dussaigne *et al.* reported the GaN grown on (111) SCD substrate by ammonia-source molecular beam epitaxy (NH_3-MBE) using an AlN buffer layer [52]. The reflectance high energy electron diffraction (RHEED) pattern demonstrated the good quality and smooth surface. The wurtzite-structured GaN grown on (111) diamond was with [0001] crystallographic direction. The root mean square roughness from atomic force microscopy (AFM) was 1.3 nm, while the surface was still with the grain boundary morphology. In addition, the cracks were observed for the 1 μm-thick GaN layer. The full-width at half maximum (FWHM) of the XRD rocking curve around (002)-plane was 1500 arcsec. For the GaN grown on the (111) orientated SCD substrate, the films has an in-plane epitaxial relationship [10-10] GaN//[110] diamond. The pre-treatments of the diamond surface were helpful to eliminate the formation of the amorphous layer or the inversion domains [53]. In 2010, Dussaigne *et al.* used a strain engineered interlayer to improve the surface morphology of the GaN grown on the (111) SCD substrate by MBE using ammonia as nitrogen source [54]. This strain engineered interlayer composed of a sequence of 200-nm-thick AlN layer and 200 nm-thick GaN layer. The rms of the 800 nm-thick GaN epitaxial layer was reduced to 0.6 nm, and no cracks were observed on the

surface. The mobility of the 2DEG was improved to be 750 cm^2/Vs with the sheet carrier density of 1.4×10^{13} cm^{-2} from the AlGaN/GaN heterojunction, as shown in Figure 7. For the HEMT devices, the 200 nm gate length devices showed 0.73 A/mm maximum drain current

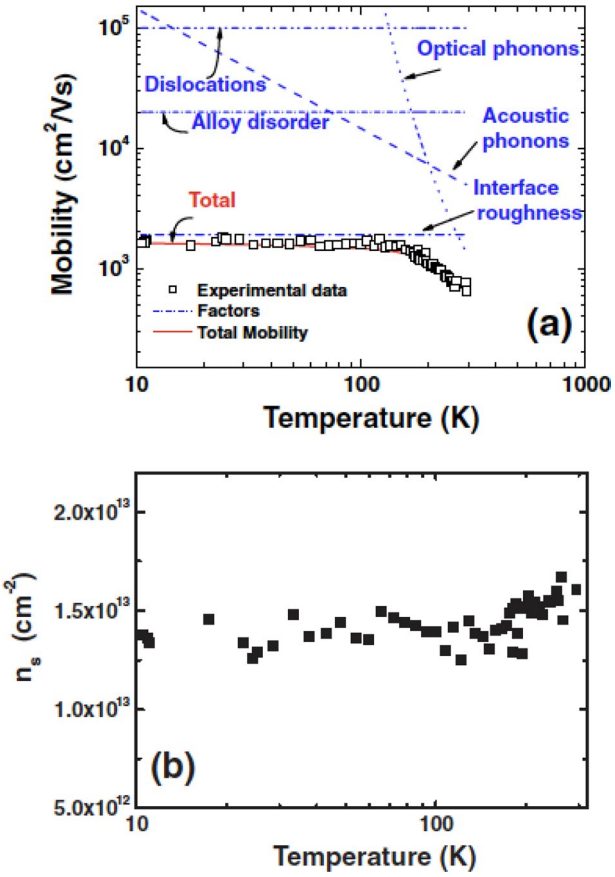

Figure 7. Temperature dependent Hall effect measurements: (a) experimental data (opened squares) together with calculated electron mobility considering different limiting factors (blue dashed/dotted lines) and (b) sheet carrier density [54].

density and f_T and f_{max} cut-off frequency of 21 and 42 GHz [55].

The progress of GaN grown on the SCD (111) substrates was also achieved by the NTT Basic Research Laboratories. In 2011, Hirama *et al.* reported the AlGaN/GaN HEMTs with a low thermal resistance grown on SCD (111) substrate by using MOCVD [56]. Benefitting from a high temperature cleaning process at 1200 °C in the hydrogen ambient, the formation of the amorphous interfacial layer was prevented on the diamond substrate, which was a crucial process to obtain the atomically abrupt AlN/diamond heterointerface [57]. After the thermal cleaning, a 180 nm-thick AlN buffer was grown, followed by 20-period AlN/GaN multilayers, then the AlGaN/GaN heterostructure was grown with the GaN thickness of 600 nm. Although the surface morphology did not show atomic steps, the metal-polar was confirmed for the structure using convergent beam electron diffraction in this study. The two-dimensional electron gas (2DEG) was successfully achieved, with the sheet carrier density of 1.0×10^{13} cm^{-2} and mobility of 730 cm^2/Vs. The AlGaN/GaN HEMTs with a 3 µm-gate length showed the maximum drain current of 220 mA/mm, cut-off frequency of 3 GHz and maximum frequency of oscillation of 7 GHz. The thermal resistance between HEMT and diamond is 4.1 K mm/W, as shown in Figure 8. The 0.4 µm-gate-length HEMT showed a dc drain-current density of 770 mA/mm and breakdown voltage of 165 V [58]. The RF power density of 2.13 W/mm was obtained (Figure 9). This is the first report on the RF power operation of the AlGaN/GaN HEMTs epitaxially grown on the diamond substrate.

The nano-crystalline and poly-crystalline diamond were also proposed as the template for the epitaxial growth of GaN to achieve the effective thermal

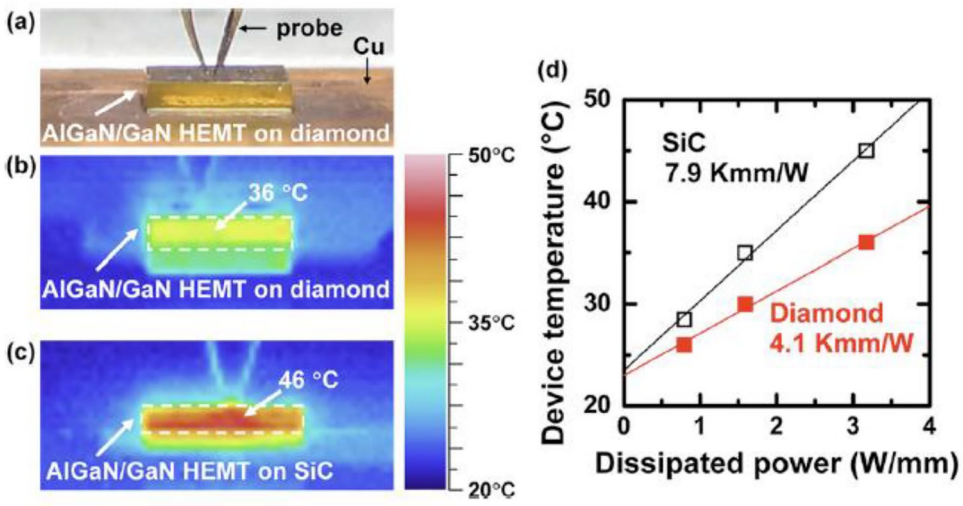

Figure 8. (a) Setup for measuring the temperature distributions from the side of the AlGaN/GaN HEMTs on the diamond or SiC substrates. Temperature distribution of the AlGaN/GaN HEMTs on (b) diamond and (c) SiC substrates at a dissipated power of 2 W (3.2 W/mm). (d) Dissipated power dependence of device temperature for AlGaN/GaN HEMTs on the diamond and SiC substrates. Closed and open squares indicate the temperatures for diamond and SiC substrates, respectively [56].

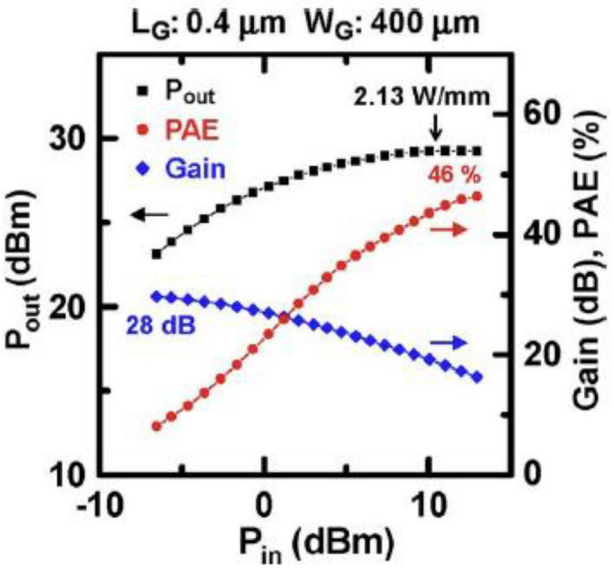

Figure 9. RF large-signal characteristics of an AlGaN/GaN HEMT at 1 GHz [58].

dissipation [60–63]. The diamond was firstly deposited on the silicon substrate, therefore, there is no limitation in the substrate size. A low-temperature buffer layer is typically utilized before the deposition of GaN films. Unfortunately, the GaN layer was not pure wurtzite structure and the polycrystalline form was typically observed [60–62]. Recently, an epitaxial lateral overgrowth (ELO) of single-crystalline thick GaN films were reported on the polycrystalline diamond [63]. The polycrystalline diamond was deposited on the GaN/Si wafers using hot filament CVD. The GaN was grown on the window region between the diamond stripes. A lower pressure, higher V/III ratio, higher temperature, and GaN window mask openings along [1$\bar{1}$00] resulted in enhanced lateral growth of GaN. Complete lateral coverage and coalescence of GaN were achieved over a [1$\bar{1}$00]-oriented 5 µm-wide GaN window between 5 µm diamond stripes. The advantage of the ELO growth is no interlayer formation between diamond and GaN, which will be promising for the effective thermal dissipation. However, there is no device demonstration or the TBR_{eff} results from this technique.

The interface thermal property was analyzed for the HEMT device epitaxially grown on the SCD substrate by N-plasma MBE [64]. A transient interferometric method, in combination with a three-dimensional model, was used to describe a pulsed operation of a transistor-like heater, and a micro-Raman technique was used in a steady state. The thermal conductivity of the diamond was found to be 2200 W/mK, and a relatively lower TBR_{eff} of < 10 m^{2}K/GW was achieved. The temperature increase in the device was saturated after 1 μs from the start of the heat dissipation and the normalized device thermal resistance of about 3.5 K mm/W was achieved.

4. Diamond epitaxially grown on GaN wafers

The uniqueness of the direct CVD diamond growth on GaN is that the diamond can be deposited as close as possible to the Joule heating location of the HEMTs. This approach is highly effective for the thermal dissipation of HEMTs. However, there are three limitations that restrict this technique. First, the presence of hydrogen during the growth of CVD diamond requires a dielectric layer such as SiN_x utilized to protect GaN layer, contributing to the large TBR_{eff} for the devices [65]. Second, the diamond nucleating layer begins with many small grains, resulting in a poor thermal conductivity [66]. Third, to avoid the degradation of the GaN, low temperature deposition is needed. However, it has been shown that lowering temperature below 600 °C using conventional H_2/CH_4 based growth results in the growth of the poor-quality diamond [67]. In addition, the stress is another unavoidable problem. In general, diamond will only nucleate on the carbide forming materials like many refractory metals or Si and will not outgrow in the single crystal phase even on cubic substrates (except for growth on Ir [68]). There is no report on the SCD deposited on GaN, as an alternative, the nano-crystalline or poly-crystalline diamond were fabricated [36, 69].

The first attempt to deposit diamond films onto hexagonal GaN was by the group of Oba and Sugino [46, 70], who deposited diamond on (0001)-oriented GaN films using microwave plasma CVD. To prevent the etching to the GaN surface, a carburiziation was conducted. The growth of oriented, heteroepitaxial isolated diamond crystals on the GaN surface was achieved, but the crystals did not coalesce into a continuous film due to the low nucleation density. In 2006, May *et al.* reported the growth of continuous layers of diamond on GaN using a hot filament CVD technique [67]. They found that there was a competition between the rate of diamond deposition and the rate of GaN decomposition, which determined whether net deposition or etching occurred. When the temperature was higher than 600 °C, the GaN decomposed, evolving gaseous N_2 which created pinholes in the growing diamond layer or caused it to delaminate. Lowering the substrate temperature below 600 °C resulted in a prohibitively low growth rate and poor-quality diamond.

The earliest pieces of diamond-on-GaN wafer were obtained by growing the poly-crystalline diamond on a dielectric-coated Ga-face GaN-on-Si wafer, then the Si was etched away, leaving behind an N-face GaN-on-diamond wafer [71]. The thickness of the CVD poly-crystalline diamond was 25 µm. By 2006, the Ga-face GaN-on-diamond HEMT was obtained. In this process, firstly the GaN-on-Si epitaxy was bonded onto a temporary Si carrier, then the host Si substrate was etched away, followed by the deposition of a 50 nm-thick

dielectric (such as SiN_x) onto the exposed rear of the GaN. The polycrystalline diamond was finally deposited onto the dielectric for the GaN-on-diamond HEMT devices by using a hot filament CVD process. The wafer size at that time was over $10 \times 10\,mm^2$ area, and the epi-surface exhibited countless particulates that obstructed device processing. The electrical current collapse for the first HEMT on diamond was observed. In 2012, the thickness of the polycrystalline diamond was increased to 100 μm [72], and the device performance was further improved [73]. Over 7 W/mm output power density at 10 GHz was reported, along with the peak PAE over 46% and power gain over 11 dB at 40 V.

In the above process of diamond deposited on GaN, the residual stress was propagated into the GaN layer and caused local defects and uneven bonding of the wafer after the carrier wafer was removed, leading to the wafer bow and warp. The interaction between the intrinsic stress and the built-in stress in the GaN affected the electrical behavior of the device. The effects of the increased stress represent a significant reliability concern for the device, especially when considering the function and life time of the device [43, 74–78]. Jia *et al.* utilized a double-sided diamond deposition technique to reduce the stress problems [79]. A tensile stress of ~0.5 GPa was obtained in the GaN layer of the GaN-on-diamond structure, and the crystal quality of the GaN was observed to not change significantly after the wafer transfer process. A seamless interface with *a* ~10 nm SiC and a thin Al-Si–N intermediate interfacial layer were observed, which facilitated the adhesion between the GaN and the heat dissipation diamond layer. However, the interfacial layer may lead to a high TBR_{eff}. Zhou *et al.* investigated the interface thermal property of GaN and polycrystalline diamond with SiN_x and AlN barrier layers as well as without any barrier layer [80,81] (Figure 10). The TBR_{eff} was estimated by TDTR method with a 100 nm-thick Au as the transducer layer, which had a value of ~ $6.5\,m^2$ K/GW when an ultrathin SiN barrier layers were utilized. The direct growth of diamond onto GaN results in one to two orders of magnitude higher TBR_{eff} due to the formation of a rough interface. AlN barrier layers can produce a TBR_{eff} as low as that with SiN_x barrier layers in some cases. However, the TBR_{eff} is rather dependent on growth conditions. A decreasing diamond thermal resistance with increasing growth temperature was also observed. To compensate the thermal stress between GaN and diamond during the epitaxial growth, Cuenca and Smith proposed a membrane-based technology [35, 82]. From their analysis based on the analytical models, the bow for a membrane structure with small sizes were underestimated and the bow could be reduced if the membrane was pre-stressed to become flat at CVD temperatures. The

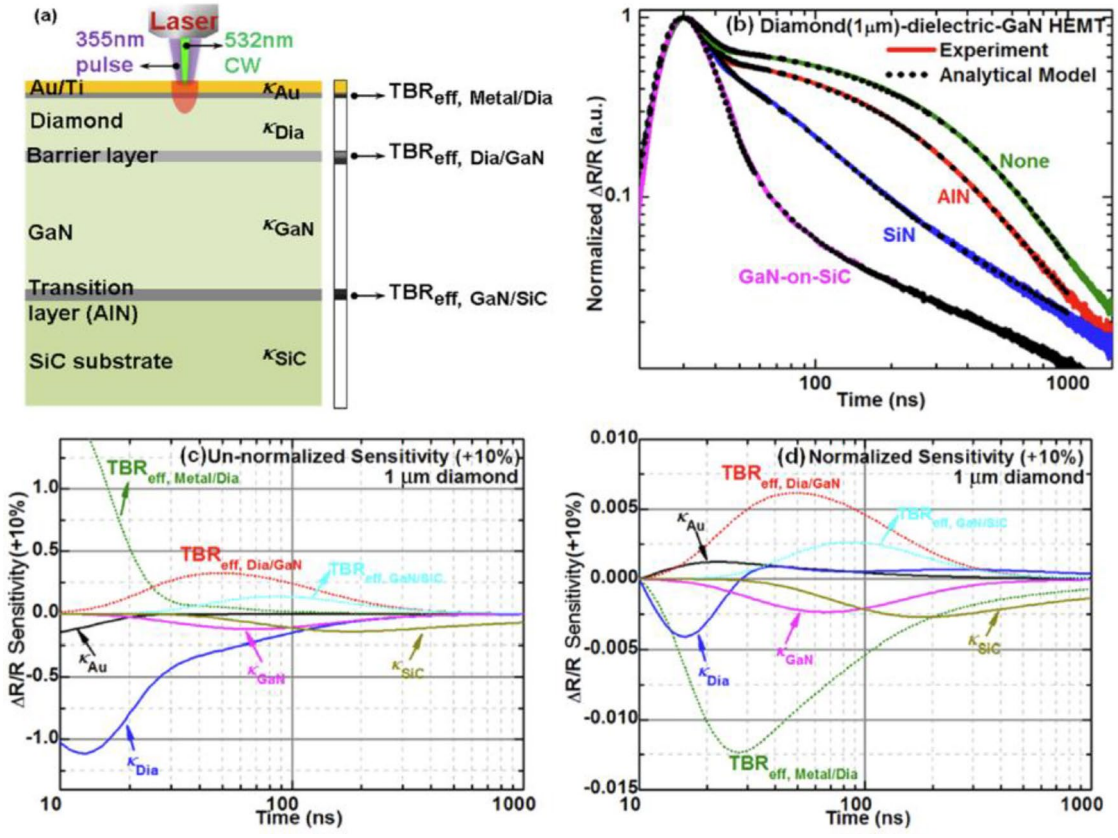

Figure 10. (a) sample structure and thermoreflectance measurement scheme. (b) Thermoreflectance signal as as function of time of GaN-on-diamond samples with different barrier layer. Lines represent the experimental value and dots represent an analytical model fitted to the experimental values. (c) Unnormalized and (b) normalized sensitivity curves for the GaN-SiN-diamond samples, with the sensitivity of $\triangle R/R$ corresponding to ±10% change in each input parameter in the model. The laser heating pulse stops at 10 ns [80].

sample was from the GaN-on-Si. The Si substrate was selectively removed, and the windows were formed for the polycrystalline diamond deposition using microwave plasma CVD. The diamond was grown on the etched exposed N-polar AlN epitaxial nucleation layers. The high-quality diamond/voi-free AlN interfaces were confirmed from microstructure analysis. This approach is the important demonstration to solve the thermal stress issue during the epitaxial growth of diamond heat spreader on the GaN-based materials and devices.

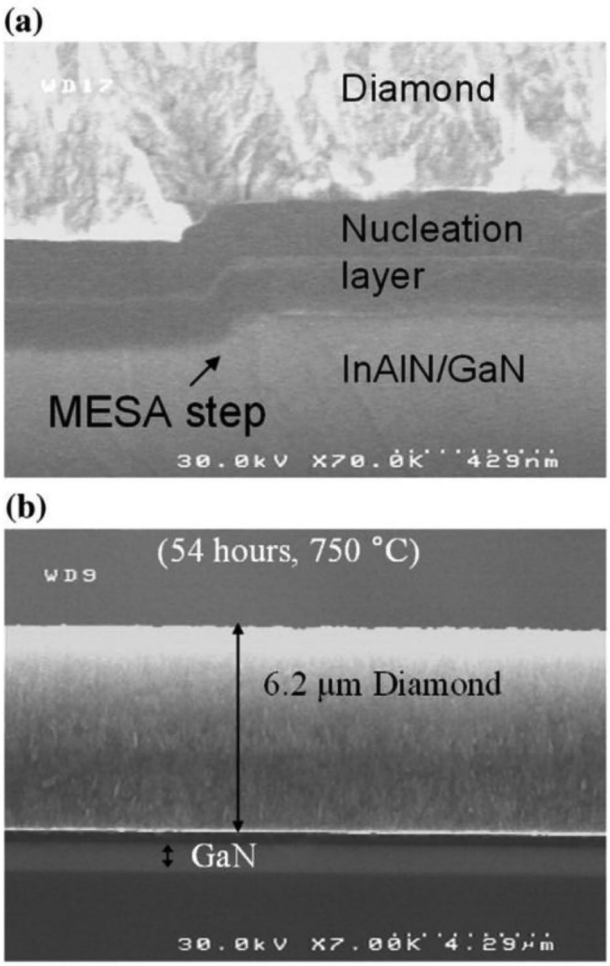

Figure 11. (a) The NCD growth was conformal across MESA edges and (b) no cracking or blistering of the growth NCD films even for films as thick as 6.2 µm.

The nanocrystalline diamond (NCD) films deposited on the fabricated InAlN/GaN HEMTs devices were reported in 2011 by Alomari *et al.* [83] (Figure 11). The thermally stable contacts were prepared by depositing a Ta diffusion barrier on the Cu contacts. Then the HEMTs structure were passivated with a thin Si based interlayer (containing the passivated layer and Si-nucleation layer). The NCD nucleation and growth steps were conducted in a hot filament CVD chamber at 750-770 °C. A nucleation density of about 3×10^{10} nuclei/cm^2 was achieved. The average grain size on the top was around 120 nm in diameter. Raman spectroscopy indicated a dominant diamond peak as the main constituent while the presence of the graphitic phase at the grain boundaries. No degradation or change in the HEMT DC characteristics was observed despite the high temperature of the diamond overgrowth process. Tadjer *et al.* reported the NCD-capped HEMTs exhibited approximately 20% lower device temperature from 0.5 to 9 W/mm dc power device operation [84]. NCD-capped HEMTs exhibited the improved carrier density and sheet resistance, but the on-state resistance and the breakdown behaviors were degraded, as shown in Figure 12. The selective growth of the NCD was reported by Ahmed et al. [65] on the AlGaN/GaN wafer by hot filament CVD. A thin layer of SiN_x by plasma enhanced CVD, deposited prior to seeding and diamond deposition, was found to be essential to protect the AlGaN/GaN wafer. A methane concentration of 3.0% was used to increase the diamond growth rate and faster surface coverage. Excellent selectively and minimal surface damage to AlGaN were achieved. The

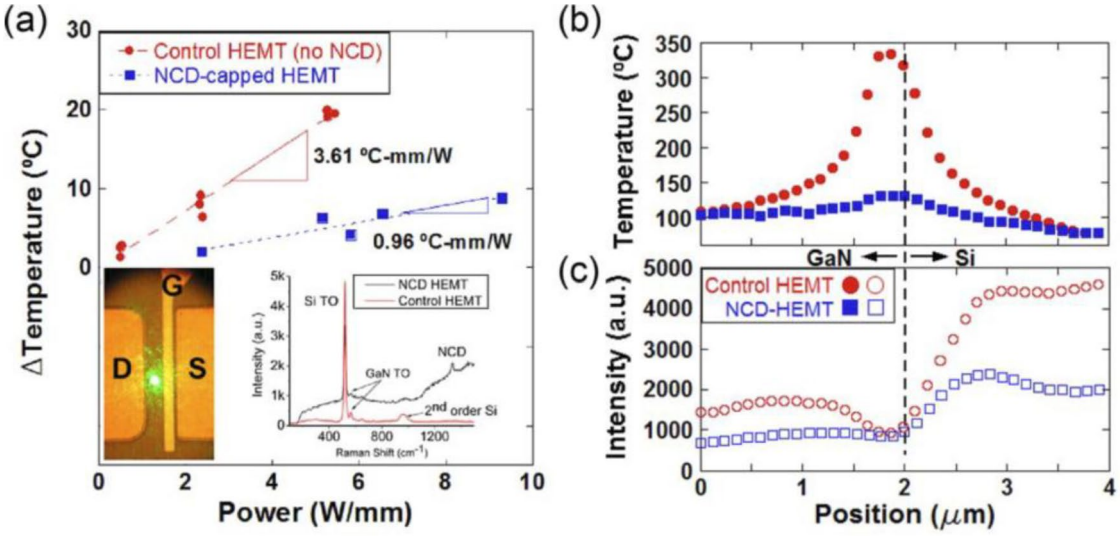

Figure 12. (a) Non-confocal Raman thermography profile of the device channel temperature of AlGaN/GaN HEMTs with and without NCD heat spreading. (b)Temperature-depth confocal Raman profile of the HEMT structures under dc bias. (c) Confocal Raman Si TO peak intensity depth profile showing the GaN/Si interface [84].

dual side deposition of the NCD was also reported with a AlN as the dielectric layer [85].

The interface thermal properties between GaN and NCD diamond were improved by Smith *et al.* using a two-step mixed-seeding method [86]. It was found that the mixture of microdiamond and nanodiamond seeding led to a low TBR_{eff}. While the diamond directly grown onto GaN was proved to be unsuccessful due to the poor adhesion. The two-step mixed-seeding method gave TBR_{eff} values lower than 6 m^2K/GW, 30 times smaller than those of films using nanodiamond seeding alone. Such remarkably low thermal barriers obtained with the mixed-seeding process of microdiamond and nanodiamond offer a promising route for the fabrication of high-power GaN HEMTs using diamond as a heat spreader.

The double-side diamond integration to the HEMTs devices were also developed to improve the heat dissipation. In 2019, Fujitsu Limited and Fujitsu Laboratories Ltd. deposited diamond films on the front surface of the HEMT device. They also bonded the SCD on the back side of HEMTs using SiC interlayer, as shown in Figure 13 [89]. The nanodiamond films were grown at a temperature of 650 °C without degrading the transistors' performance. With the NCD layer on the front side, the amount of heat generated during HEMT operation was reduced by approximately 40% compared to that without the diamond film, and the temperature can be lowered by 100 °C or more. By combining the heat dissipation from the back side of the GaN HEMT with SCD substrate, the operating temperature is expected to be reduced by approximately 77%.

5. Interface thermal property between GaN and diamond

Thermal boundary resistance is an essential concern for GaN-on-diamond transistors especially when they are operating at high-power densities. According to the diffuse mismatch model (DMM), the theoretical limits of TBR_{eff} between GaN and diamond is 3 m^2K/GW [88]. However, the measured values are far from the ideality. The interface transition layer between GaN and diamond plays a key role for the contribution of the TBR_{eff}, no matter if the GaN is bonded to diamond, epitaxially grown on diamond or the diamond grown on GaN devices. The experimental methods that typically used to determine TBR_{eff} include the TDTR technique, transient thermoreflectance (TTR) technique, and the three-dimensional (3D) Raman thermography mapping method. The principles of the TDTR and TTR methods are similar. In the TDTR measurement, a pump laser is utilized to periodically heat the sample surface and a probe laser monitor the thermal reflectivity signal of the transducer metal (Al or Au). The reflected intensity tracks the temperature change of the surface, and the normalized reflected intensity is equal to the normalized surface temperature change. Therefore, the change in the thermal reflectivity of the surface is directly proportional to the temperature change. The signal, which is picked up by a photodetector and a lock-in amplifier, is fitted with an analytical heat-transfer solution to infer the unknown parameters. The 3D Raman thermography mapping exploits the temperature induced phonon shift in a material, with respect to a reference phonon frequency measured at ambient temperature [89–92]. The stress can be simultaneously obtained by the simultaneously analyzing the multiple phonon modes [92]. By using a three-dimensional finite element thermal model, the temperature dependent thermal properties can be extracted [93]. The TBR_{eff} can also be extracted by analyzing the HEMTs device performance using the steady-state heat conduction model [94].

For the GaN or HEMT devices grown on diamond substrate, the buffer layers with the lattice-mismatched induced high-density dislocations, are the main reason for the high TBR_{eff}. In the bonding process or the diamond deposition on GaN, since the gallium does not readily form a carbide, SiN_x is typically used to form an interlayer. SiN_x has a low thermal conductivity of 1-2 W/mK, which introduces an additional thermal resistance. For the polycrystalline diamond deposited on the GaN with a SiN_x interlayer, the SiN_x contributes to most of the GaN-on-diamond interface thermal resistance, resulting in a TBR_{eff} of more than 30 m^2K/GW, adding >20% to the total device resistance [95]. In

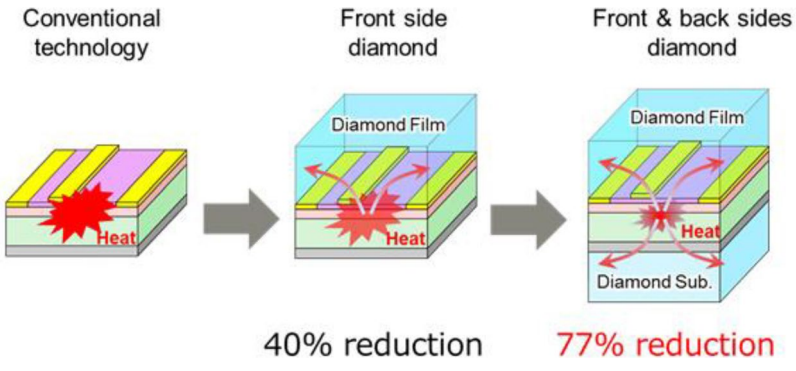

Figure 13. The heat-spreading method using the double-side diamond and the heat dissipation efficiency [87].

Table 2. Summary on the TBR_{eff} at the interface between GaN and diamond using different integration methods and different measurement methods.

Integration method	Interlayer	thickness	TBR_{eff} (m^2K/GW)	Measurement	Ref.
Direct vdW bonding	No	0	220 ± 70	TTR	[98]
RT surface-activated bonding	Si	10 nm	~18	TDTR	[43]
RT surface-activated bonding	Si	4 nm	~11		
Bonding	Thermosetting adhesion	15-20 nm	51	Device finite-element analysis	[45]
HT bonding	Adhesion	3-55 nm	27-31	TDTR	[99]
	Adhesion	3-55 nm	25-29	DC joule heating	
HT bonding	SiNx	22 nm	17	TDTR	[100]
GaN grown on SCD using MBE	Not indicated	Not indicated	<10	TDTR	[64]
Hot-filament CVD diamond on GaN	dielectric	25 nm	27	3D Raman mapping	[93]
MPCVD diamond on GaN	dielectric	50 nm	36		
CVD polycrystalline diamond grown on GaN	SiN	100 nm	38.5 ± 2.4	TDTR	[101]
CVD polycrystalline diamond grown on GaN	AlN	100 nm	56.4 ± 5.5		
CVD diamond on GaN	dielectric	50 nm	18	Raman	[102]
CVD diamond on GaN	SiNx	30 nm	29	TDTR	[103]
CVD diamond on GaN	SiNx	28 nm	12	TTR	[95]
CVD diamond on GaN	SiNx	~5 nm	<10	TDTR	[105]
CVD diamond on GaN	SiNx	~5 nm	6.5	TTR	[81]
CVD diamond on GaN	SiC	~ 5 nm	30 ± 5.5	TTR	[104]
CVD Mixed-size diamond seeding on GaN	No	0	<6	TTR	[86]

addition, the diamond nucleation layer is usually composed of a few 10 s of nm poor-quality, small-grained diamond [96], which also contributed to the TBR_{eff}. The direct diamond growth on GaN or bonding to the GaN layer usually shows much weaker interfaces, although there are rare reports on TBR_{eff} assessments. It is generally known that weaker interface results in higher TBR_{eff} [97,98]. Table 2 summarizes the reported TBR_{eff} at the GaN-on-diamond interface using different integration methods and different measurement methods.

6. Summary and outlook

In this paper, the fabrication of GaN-on-diamond wafers using different methods and the properties of the materials and the fabricated HEMT devices are systematically reviewed. The bonding of GaN or the well-fabricated AlGaN/GaN HEMTs device with diamond can maintain the quality of both the GaN devices and diamond substrate. However, the dielectric interlayers are necessary for either the high-temperature or room-temperature bonding along with an amorphous layer induced by the surface activation. This interlayer impedes the heat flow from the device channel, leading to a large TBR_{eff}. The growth technique of the GaN or AlGaN/GaN HEMTs structures on the SCD substrates were developed in recent years. A relatively lower TBR_{eff} <10 m^2K/GW was reported at the interface between epitaxial GaN and diamond substrate. However, although the HEMTs devices are demonstrated, the crystalline quality of the material and the mobility of the HEMT devices are still far from those grown on the conventional substrates of sapphire, Si, SiC and free-standing GaN substrates due to the large lattice mismatch and thermal mismatch. The CVD growth of the polycrystalline or nanocrystalline diamond on the GaN or HEMTs devices has the uniqueness of the direct growth as close as possible to the Joule hot spots, which may be highly effective for the thermal dissipation. However, the damage to the GaN by hydrogen during CVD growth and the less nucleation of the diamond restrict the film quality, leading to a poor thermal conductivity of diamond and large TBR_{eff}. In addition, the large thermal expansion coefficient between diamond and GaN results in the stress problems in the GaN-on-diamond wafers, leading to the layer cracking and wafer bow and impact the electrical performance of the devices. Up to now, a variety of efforts have been performed to challenge the above problems with different methods. Without doubt, the heat dissipation using diamond as heat spreader for the AlGaN/GaN HEMTs devices is a highly effective way to reduce the operation junction temperature compared to the devices on sapphire, Si and SiC substrates. Although the large TBR_{eff} exists between GaN and diamond, Fujitsu laboratory has reduced the device temperature during HEMT operation by more than 40%, and the temperature can be lowered by 100 °C or more due to the high thermal conductivity of diamond [87]. Nevertheless, to take the full advantage of the GaN technology for the high-power applications, the reduction of the TBR_{eff} between GaN and diamond is still a challenge. Novel strategies and concepts are still required for the effective thermal management of GaN-based power devices using the diamond heat spreader.

Disclosure statement

No potential conflict of interest was reported by the author.

Funding

This work was supported by the JST-PRESTO Grant No. JPMJPR19I7, and World Premier International Research Center (WPI) initiative on Materials Nanoarchitectonics (MANA), Ministry of Education, Culture, Sports, Science & Technology (MEXT) in Japan, and National Key Research and Development Program of China (No.2018YFE0125700).

Notes on contributor

Dr. Liwen Sang is the Independent Scientist at the International Center for Materials Nanoarchitectonics (MANA) in National Institute for Materials Science (NIMS), in Japan. She is also the JST-PRESTO researcher under the support of Precursory Research for Embryonic Science and Technology (PRESTO) program, Japan Science and Technology Agency. After receiving her Ph.D degree in Physics from Peking University, she went to NIMS, Japan as the postdoctoral researcher, and then was promoted to the permanent position in NIMS. Her current research interest is the interface engineering for III-V nitride materials and devices.

References

[1] Millan J, Godignon P, Perpina X, et al. A survey of wide bandgap power semiconductor devices. IEEE Trans Power Electron. 2014; 29(5):2155–2163.
[2] Sang LW, Ren B, Endo E, et al. Boosting the doping efficiency of Mg in p-GaN grown on the free-standing GaN substrates. Appl Phys Lett. 2019; 115(17):172103.
[3] Mishra UK, Shen L, Kazior TE, et al. GaN-based RF power devices and amplifiers. Proc IEEE. 2008; 96(2):387–305.
[4] Ren B, Liao M, Sumiya M, et al. Nearly ideal vertical GaN Schottky barrier diodes with ultralow turn-on voltage and on-resistance. Appl Phys Express. 2017; 10(5):051001.
[5] Zhang K, Sumiya M, Liao M, et al. P-channel InGaN/GaN heterostructure metal-oxide-semiconductor field effect transistor based on polarization-induced two-dimensional hole gas. Sci Rep. 2016; 6(1):23683.
[6] Ambacher O. Growth and applications of group III nitrides. J Phys D Appl Phys. 1998; 31(20):2653–2710.
[7] Mohammad SN, Morkoc H. Progress and prospects of group-III nitride semiconductors. Prog Quantum Electron. 1996; 20(5-6):361–525.
[8] Mishra UK, Parikh P, Wu YF. AlGaN/GaN HEMTs-an overview of device operation and applications. Proc IEEE. 2002; 90(6):1022–1031.
[9] He JQ, Cheng WC, Wang Q, et al. Recent advances in GaN-based power HEMT devices. Adv Electron Mater. 2021; 7(4):2001045.
[10] Pengelly RS, Wood SM, Milligan JW, et al. A review of GaN on SiC high electron-mobility power transistors and MMICs. IEEE Trans Microwave Theory Techn. 2012; 60(6):1764–1783.
[11] Wu YF, Kapolnek D, Ibbetson JP, et al. Very-high power density AlGaN/GaN HEMTs. IEEE Trans Electron Dev. 2001; 48(3):586–590.
[12] Amano H, Baines Y, Beam E, et al. The 2018 GaN power electronics roadmap. J Phys D Appl Phys. 2018;51(16):163001.
[13] Francis D, Wasserbauer J, Faili F, et al. GaN HEMT epilayers on diamond substrates. In: CS MANTECH Conference, May 14-17; Austin, Texas, USA; 2007.
[14] Shibata H, Waseda Y, Ohta H, et al. High thermal conductivity of gallium nitride (GaN) crystals grown by HVPE process. Mater Trans. 2007; 48(10):2782–2786.
[15] Wei R, Song S, Yang K, et al. Thermal conductivity of 4H-SiC single crystals. J Appl Phys. 2013;113(5):053503.
[16] Liao M, Shen B, Wang Z. Ultra-wide bandgap semiconductor materials. Oxford (UK): Elsevier; 2019.
[17] Inyushkin AV, Taldenkov AN, Ralchenko VG, et al. Thermal conductivity of high purity synthetic single crystal diamonds. Phys Rev B. 2018; 97:144305.
[18] Wort CJH, Sweeney CG, Cooper MA, et al. Thermal properties of bulk polycrystalline CVD diamond. Diamond Relat Mater. 1994; 3(9):1158–1167.
[19] Liao M. Progress in semiconductor diamond photodetectors and MEMS sensors. Functional Diamond. 2021; 1:1(1):29–46.
[20] Nochetto HC, Kankowski NR, Bar-Cohen A. GaN HEMT junction temperature dependence on diamond substrate anisotropy and thermal boundary resistance. In: 34th IEEE CSIC Symposium, Oct 14-17; La Jolla, CA; 2012. p. 1–4.
[21] Salm RP. In thermal modelling of GaN HEMTs on sapphire and diamond in a MSEE Thesis document, Naval Postgraduate School, Monterey, CA; Dec 2005.
[22] Mcglone D, Weatherford T, Gillespie J, et al. Electrical and thermal modelling of AlGaN/GaN HEMTS on diamond silicon substrates. In: IEEE ROCS Workship, Monterey, CA, USA; 2008. p. 3–14.
[23] Ejeckam F, Francis D, Faili F, et al. GaN-on-Diamond wafers: a progress report. In: GOMACTech Mar 31-Apr 4, 2014. Conference Proceedings.
[24] Gabler J, Pleger S. Precision and micro CVD diamond-coated grinding tools. Int J Mach Tools Manuf. 2010; 50(4):420–424.
[25] von Witzendorff P, Moalem A, Kling R, et.al. Laser dressing of metal bonded diamond blades for cutting of hard brittle materials. J Laser Appl. 2012; 24(2):022002.
[26] Zeren M, Karagoz S. Sintering of polycrystalline diamond cutting tools. Mater Des. 2007; 28(3):1055–1058.
[27] Sexton TN, Cooley CH. Polycrystalline diamond thrust bearings for down-hole oil and gas drilling tools. Wear. 2009;267(5-8):1041–1045.
[28] Schuelke T, Grotjohn TA. Diamond polishing. Diamond Relat Mater. 2013; 32:17–26.
[29] Zhu ZH, Ejeckam FE, Qian Y, et al. Wafer bonding technology and its applications in optoelectronic devices and materials. Quantum Electron IEEE J. 1997; 3(3):927–936.
[30] Liau ZL, Mull DE. Wafer fusion. A novel technique for optoelectronic device fabrication and monolithic integration. Appl Phys Lett. 1990; 56(8):737–739.
[31] Kelly MK, Ambacher O, Dimitrov R, et al. Optical process for liftoff of group III-nitride films. Phys Stat Sol A. 1997;159(1):R3–R4.
[32] Dadgar A, Blasing J, Diez A, et al. Metalorganic chemical vapor epitaxy of crack-free GaN on Si (111) exceeding 1 mum in thickness. Jpn J Appl Phys. 2000; 39(Part 2, No. 11B):L1183–L1185.
[33] Ikeda N, Niiyama Y, Kambayashi H, et al. GaN power transistors on Si substrates for switching applications. Proc IEEE. 2010; 98(7):1151–1161.
[34] Francis D, Faili F, Babić D, et al. Formation and characterization of 4-inch GaN-on-diamond substrates. Diamond Relat Mater. 2010; 19(2-3):229–233.
[35] Cuenca JA, Smith MD, Field DE, et al. Thermal stress modelling of diamond on GaN/III-Nitride membranes. Carbon. 2021; 174:647–661.

[36] Francis D, Wasserbauer J, Faili F, et al. GaN-HEMT epilayers on diamond substrates: recent progress. In: Proc. CS Mantech., May 14–17; Austin, TX; 2007. p. 133–136.
[37] Diduck Q, Felbinger J, Eastman LF, et al. Frequency performance enhancement of AlGaN/GaN HEMTs on diamond. Electron Lett. 2009; 45(14):758–759.
[38] Felbinger JG, Chandra S, Sun Y, et al. Comparison of GaN HEMTs on diamond and SiC substrates. IEEE Electron Device Lett. 2007;28(11):948–950.
[39] Kim JC, Lee J, Kim J, et al. Challenging endeavor to integrate gallium and carbon via direct bonding to evolve GaN on diamond architecture. Scr Mater. 2018; 142:138–142.
[40] He R, Fujino M, Yamauchi A, et al. Combined surface activated bonding technique for low-temperature Cu/dielectric hybrid bonding. ECS J Solid State Sci Technol. 2016; 5:419–424.
[41] Wang C, Wang Y, Tian Y, et al. Room-temperature direct bonding of silicon and quartz glass wafer. Appl Phys Lett. 2017; 110(22):221602.
[42] Mu FW, He R, Suga T. Room temperature GaN-diamond bonding for high-power GaN-on-diamond devices. Scr Mater. 2018;150:148–151.
[43] Cheng Z, Mu FW, Yates L, et al. Interfacial thermal conductance across room-temperature-bonded GaN/diamond interfaces for GaN-on-diamond devices. ACS Appl Mater Interfaces. 2020;12(7):8376–8384.
[44] Chao PC, Chu K, Creamer C, et al. Low- temperature bonded GaN-on-diamond HEMTs with 11 W/mm output power at 10 GHz. IEEE Trans Electron Devices. 2015; 62(11):3658–3664.
[45] Liu T, Kong Y, Wu L, et al. 3-inch GaN-on-Diamond HEMTs with device-first transfer technology. IEEE Electron Device Lett. 2017; 38(10):1417–1420.
[46] Oba M, Sugino T. Oriented growth of diamond on (0001) surface of hexagonal GaN. Diamond Relat Mater. 2001;10(3-7):1343–1346.
[47] Amano H, Sawaki N, Akasaki I, et al. Metalorganic vapor phase epitaxial growth of a highly quality GaN film using an AlN buffer layer. Appl Phys Lett. 1986;48(5):353–355.
[48] Akasaki H, Amano Y, Koide K, Hiramatsu, et al. Effects of ain buffer layer on crystallographic structure and on electrical and optical properties of GaN and Ga1-xAlxN ($0 < x \leqq 0.4$) films grown on sapphire substrate by MOVPE. J Cryst Growth. 1989;98:209.
[49] Hageman PR, Schermer JJ, Larsen PK. GaN growth on single-crystal diamond substrates by metalorganic chemical vapour deposition and hydride vapour deposition. Thin Solid Films. 2003;443(1-2):9–13.
[50] Miskys CR, Garrido JA, Nebel CE, et al. AlN/diamond heterojunction diodes. Appl Phys Lett. 2003; 82(2):290–292.
[51] van Dreumel GWG, Tinnemans PT, van den Heuvel AAJ, et al. Realising epitaxial growth of GaN on (001) diamond. J App Phys. 2011;110(1):013503.
[52] Dussaigne A, Malinverni M, Martin D, Castiglia A, et al. GaN grown on (111) single crystal diamond substrate by molecular beam epitaxy. J Cryst Growh. 2009;311(21):4539–4542.
[53] Pécz B, Tóth L, Barna A, et al. Structural characteristics of single crystalline GaN films grown on (111) diamond with AlN buffer. Diamond Relat Mater. 2013; 34:9–12.
[54] Dussaigne A, Gonschorek M, M, Malinverni M, et al. High-Mobility AlGaN/GaN two-dimensional electron gas heterostructure grown on (111) single crystal diamond substrate. Jpn J Appl Phys. 2010;49(6): 061001.
[55] Alomari M, Dussaigne A, Martin D, et al. AlGaN/GaN HEMT on (111) single crystalline diamond. Electron Lett. 2010; 46(4):299–301.
[56] Hirama K, Taniyasu Y, Kasu M. AlGaN/GaN high-electron mobility transistors with low thermal resistance grown on single-crystal diamond (111) substrates by metalorganic chemical vapor-phase epitaxy. Appl Phys Lett. 2011; 98(16):162112.
[57] Hirama K, Taniyasu Y, Kasu M. Heterostructure growth of a single-crystal hexagonal AlN (0001) layer on cubic diamond (111) surface. J Appl Phys. 2010; 108(1):013528.
[58] Hirama K, Taniyasu Y, Kasu M, et al. Power operation of AlGaN/GaN HEMTs epitaxially grown on diamond. IEEE Electron Device Lett. 2012; 33(4):513–515.
[59] Zhang D, Bian JM, Qin FW, et al. Highly c-axis oriented GaN films grown on free-standing diamond substrates for high-power devices. Mater Res Bull. 2011;46(10):1582–1585.
[60] van Dreumel GW G, Buijnsters JG, Bohnen T, et al. Growth of GaN on nano-crystalline diamond substrate. Diamond Relat Mater. 2009;18(5-8):1043–4047.
[61] Polyakov A, Markov AV, Duhnovsky MP, et al. GaN epitaxial films grown by hydride vapor phase epitaxy on polycrystalline chemical vapor deposition diamond substrates using surface nanostructuring with TiN or anodic Al oxide. J Vac Sci Technol B. 2010;28(5):1011–1015.
[62] van Dreumel GW G, Bohnen T, Buijnsters JG, et al. Comparison of GaN and AlN nucleation layers for the oriented growth of GaN on diamond substrates. Diamond Relat Mater . 2010;19(5-6):437–440.
[63] Raju A, Siddique A, Anderson J, et al. Integration of GaN and diamond using epitaxial lateral overgrowth. ACS Appl Mater Interfaces. 2020; 12:39397–39404.
[64] Kuzmik J, Bychikhin Pogany D, Pichonat E, et al. Thermal characterization of MBE-grown GaN/AlGaN/GaN device on single crystalline diamond. J App Phys. 2011;109(8):086106.
[65] Ahmed R, Siddique A, Anderson J, et al. Selective area deposition of hot filament CVD diamond on 100 Mm MOCVD grown AlGaN/GaN wafers. Cryst Growth Des. 2019;19(2):672–677.
[66] Graebner JE, Jin S, Kammlott GW, et al. Large anisotropic thermal conductivity in synthetic diamond films. Nature. 1992;359(6394):401–403.
[67] May PW, Tsai HY, Wang WV, et al. Deposition of CVD diamond onto GaN. Diamond Relat Mater . 2006;15(4-8):526–530.
[68] Bauer T, Gsell S, Hörmann F, et al. Surface modifications and the first stages of heteroepitaxial diamond growth on iridium. Diamond Relat Mater. 2004;13(2):335–341.
[69] Goyal V, Sumant AV, Teweldebrhan D, et al. Direct low-temperature integration of nanocrystalline diamond with GaN substrates for improved thermal management of high-power electronics. Adv Funct Mater. 2012;22(7):1525–1530.
[70] Oba M, Sugino T. Growth of (111)-oriented diamond grains on hexagonal GaN. Jpn J Appl Phys. 2000; 39(Part 2, No. 12A):L1213–L1215.
[71] Ejeckam F, Francis D, Faili F, et al. GaN-on-diamond: a brief history. In: 2014 Lester Eastman Conference on High Performance Devices (LEC).
[72] Engdahl C. Development of high quality, tailored CVD diamond using hot filaments. Finer Points Super-Abrasive Ind. Rev. 2012, summer:22–24.
[73] Dumka DC, Chou TM, Faili F, et al. AlGaN/GaN HEMTs on diamond substrate with over 7W/mm out-

put power density at 10 GHz. Electron Lett. 2013; 49(20):1298–1299.
[74] Wang A, Tadjer MJ, Anderson TJ, et al. Impact of intrinsic stress in diamond capping layers on the electrical behavior of AlGaN/GaN HEMTs. IEEE Trans Electron Devices. 2013; 60(10):3149–3156.
[75] Kang BS, Kim S, Kim J, et al. Effect of external strain on the conductivity of AlGaN/GaN high-electron-mobility transistors. Appl Phys Lett. 2003; 83(23):4845–4847.
[76] Azize M, Palacios T. Effect of substrate-induced strain in the transport properties of AlGaN/GaN heterostructures. J Appl Phys. 2010; 108(2):023707.
[77] Jeon CM, Lee JL. Effects of tensile stress induced by silicon nitride passivation on electrical characteristics of AlGaN/GaN heterostructure field-effect transistors. Appl Phys Lett. 2005; 86(17):172101.
[78] Ahmad I, Holtz M, Faleev NN, et al. Dependence of the stress-temperature coefficient on dislocation density in epitaxial GaN grown on a-Al2O3 and 6H-SiC substrates. J Appl Phys. 2004;95(4):1692–1697.
[79] Jia X, Wei JJ, Huang YB, et al. Fabrication of low stress GaN-on-diamond structure via dual-sided diamond film deposition. J Mater Sci. 2021;56(11):6903–6911.
[80] Zhou Y, Anaya J, Pomeroy J, et al. Barrier-layer optimization for enhanced GaN-on-diamond device cooling. ACS Appl Mater Interfaces. 2017;9(39):34416–34422.,
[81] Zhou Y, Ramaneti R, Anaya JL, et al. Thermal characterization of polycrystalline diamond thin film heat spreaders grown on GaN HEMTs. Appl Phys Lett. 2017;111(4):041901.
[82] Smith MD, Cuenca JA, Field DE, et al. GaN-on-diamond technology platform: Bonding-free membrane manufacturing process. AIP Adv. 2020;10(3):035306.
[83] Alomari M, Dipalo M, Rossi S, et al. Diamond overgrown InAlN/GaN HEMT. Diamond Relat Mater. 2011;20(4):604–608.
[84] Tadjer MJ, Anderson TJ, Hobart KD, et al. Reduced self-heating in AlGaN/GaN HEMTs using nanocrystalline diamond heat-spreading films. IEEE Electron Device Lett. 2012;33(1):23–25.
[85] Jia X, Wei JJ, Huang YB, et al. Enhancement of diamond seeding on aluminum nitride dielectric by electrostatic adsorption for GaN-on-diamond preparation. J Mater Res. 2020;35(5):508–515.
[86] Smith EJW, Piracha AH, Field D, et al. Mixed-size diamond seeding for low-thermal-barrier growth of CVD diamond onto GaN and AlN. Carbon. 2020; 167: 620–626.
[87] https://www.fujitsu.com/global/about/resources/news/press-releases/2019/1205-01.html.
[88] Cho JW, Li ZJ, Asheghi M, et al. Near-junction thermal management: thermal conduction in gallium nitride composite substrates. Annual Rev Heat Transfer. 2015; 18:7–45.
[89] Kuball M, Hayes JM, Uren MJ, Martin I, et al. Measurement of temperature in active high-power AlGaN/GaN HFETs using Raman spectroscopy. IEEE Electron Device Lett. 2002; 23(1):7–9.
[90] Sarua A, Ji HF, Hilton KP, et al. Thermal bondary resistance between GaN and substrate in AlGaN/GaN electronic devices. IEEE Trans Electron Devices. 2007; 54(12):3152–3158.
[91] Manoi A, Pomeroy JW, Killat N, Kuball M. Benchmarking of thermal boundary resistance in AlGaN/GaN HEMTs on SiC substrates: implications of the nucleation layer microstructure. IEEE Electron Device Lett. 2010; 31(12):1395–1397.
[92] Batten T, Pomeroy JW, Uren MJ, et al. Simultaneous measurement of temperature and thermal stress in AlGaN/gan high electron mobility transistors using Raman scattering spectroscopy. J. Appl.Phys. 2009; 106(9):094509.
[93] Pomeroy JW, Bernardoni M, Dumka DC, et al. Low thermal resistance GaN-on-diamond transistors characterized by three-dimensional Raman thermography mapping. Appl Phys Lett. 2014; 104(8):083513.
[94] Zhang H, Guo ZX, Lu YF. Enhancement of hot spot cooling by capped diamond layer deposition for multi-finger AlGaN/GaN HEMTs. IEEE Trans Electron Devices. 2020; 67(1):47–52.
[95] Sun HR, Simon RB, Pomeroy JW, et al. Reducing GaN-on-diamond interfacial thermal resistance for high power transistor applications. Appl Phys Lett. 2015; 106(11):111906.
[96] May PW. Diamond thin films: a 21st-century material. Phil Trans R Soc A. 2000;358(1766):473–495.
[97] Giri A, Braun JL, Hopkins PE. Implications of interfacial bond strength on the spectral contributions to thermal boundary conductance across solid, liquid, and gas interfaces: a molecular dynamics study. J Phys Chem C. 2016;120(43):24847–24856.
[98] Waller WM, Pomeroy JW, Field D, et al. Thermal boundary resistance of direct van der waals bonded GaN-on-diamond. Semicond Sci Technol. 2020; 35(9):095021.
[99] Cho JW, Li ZJ, Bozorg-Grayeli E, et al. Improved thermal interfaces of GaN-diamond composite substrates for HEMT applications. IEEE Trans Compon Packag Manufact Technol. 2013; 3(1):79–85.
[100] Cho J, Francis D, Altman DH, et al. Phonon conduction in GaN-diamond composite substrates. J Appl Phys. 2017;121(5):055105. No.
[101] Jia Z, Wei JJ, Kong YC, et al. The influence of dielectric layer on the thermal boundary resistance of GaN-on-diamond substrate. Surf Interface Anal. 2019;51(7):783–790.
[102] Dumka D, Chou T, Jimenez J, et al. Electrical and thermal performance of AlGaN/GaN HEMTs on diamond substrate for RF applications. In: IEEE Compound Semiconductor Integrated Circuit Symposium (CSICS); 2013. p. 1–4.
[103] Cho J, Won Y, Francis D, et al. Thermal interface resistance measurements for GaN-on-diamond composite substrates. In: IEEE Compound Semiconductor Integrated Circuit Symposium (CSICS); 2014. p. 1–4.
[104] Field DE, Cuenca JA, Smith M, et al. Crystalline interlayers for reducing the effective thermal boundary resistance in GaN-on-diamond. ACS Appl Mater Interfaces. 2020;12(48):54138–54145.
[105] Yates L, Anderson J, Gu X, et al. Low thermal boundary resistance interfaces for GaN-on-Diamond devices. ACS Appl Mater Interfaces. 2018; 10(28):24302–24309.